

Turbulence near initial conditions

K. Steiros*

Department of Aeronautics, Imperial College London, SW7 2AZ London, United Kingdom



(Received 17 March 2021; accepted 4 October 2022; published 19 October 2022)

Recent observations indicate that the evolution of homogenous turbulence near its initial conditions is characterized by nonclassical, out-of-equilibrium scaling laws for the energy spectrum and dissipation rate. Based on these two observations, this work derives expressions for the evolution of the kinetic energy, interscale energy flux, and integral length scale, for homogenous decaying turbulence cascades near initial conditions. As expected, the predictions differ from those of the equilibrium Kolmogorov theory. Validation is provided using data from direct numerical simulations.

DOI: [10.1103/PhysRevFluids.7.104607](https://doi.org/10.1103/PhysRevFluids.7.104607)

I. INTRODUCTION

A fundamental result of turbulence research is Kolmogorov's dissipation scaling $\epsilon = C_\epsilon u^3/L$, connecting the turbulent dissipation ϵ with the (normalized) kinetic energy of the flow u^2 and the integral lengthscale L . C_ϵ is an assumed constant, known as the dissipation coefficient [1,2]. The above scaling rests on two main assumptions [3–6]. First, that the rate of energy transfer from large to small scales can be expressed as $\Pi_a \propto u^3/L$ (the subscript a signifies that the interscale energy flux is evaluated at an eddy size r of order L). Second, that the cascade is approximately static, or in “equilibrium,” i.e., that $\Pi \approx \epsilon$ [7] (note that equilibrium is not used here in the context of the detailed balance encountered in statistical physics). Although static cascades are uncommon, the above framework is of immense importance, as it is expected that, even in highly unsteady regimes, equilibrium is an asymptotic state of the turbulent eddies, when wave numbers $k \sim 1/r$ and the global Reynolds number tend to infinity, i.e., when $r \ll L$ and $\text{Re} \rightarrow \infty$ [6]. Indeed, in such conditions, approximate equilibrium and its repercussion, the self-preserving expression for the energy spectrum known as the $-5/3$ law, i.e., $E \propto \epsilon^{2/3} L^{5/3} (kL)^{-5/3}$, have been observed [6,8].

The above two main assumptions are therefore expected to be fulfilled in unsteady cascades, albeit in different regions of space-time: the first assumption ($\Pi_a \propto u^3/L$) being valid when $r \approx L$ while the second ($\Pi \approx \epsilon$) when $r \ll L$. To bridge those and derive a “dissipation law” one would need some information on the behavior of the ratio Π_a/ϵ (evaluated at $r \approx L$). Evidently, equilibrium will be invalid at large eddies in unsteady regimes (see also the discussions in Bos *et al.* [9] and Lumley [10]), i.e., Π_a/ϵ will not be equal to unity, but will rather vary depending on the type of flow. We may thus expect a variety of dissipation scalings (i.e., nonunity C_ϵ) and departures from the equilibrium self-preserving relation $E \propto \epsilon^{2/3} L^{5/3} (kL)^{-5/3}$ at finite wave numbers.

For the particular case of homogenous decaying turbulence, Goto and Vassilicos [11] and Steiros [12] showed that, when sufficient time has passed from the onset of decay, the large scales of the cascade are out of equilibrium, but evolve in a particular self-preserving manner. This type of evolution was termed “balanced” as it was found to be caused by a proportionality of the terms of the spectral energy budget equation. Such balance leads to $\Pi_a/\epsilon = \text{const.}$, where the constant is less than unity, indicating the nonequilibrium state of the large scales (see also Ref. [9]). This

*k.steiros@imperial.ac.uk

behavior was found to create a nonequilibrium correction to Kolmogorov’s $-5/3$ law [12], while retaining the classical dissipation scaling $C_\epsilon = \text{const.}$ [11,12]. Closer to the initial conditions this “balance” is broken [12] and a reproducible nonconstant scaling $C_\epsilon \propto \text{Re}_\lambda^{-m}$, with $m \approx 1$, is instead observed [11,13–17]. The results of Goto and Vassilicos [11] suggest that this non-Kolmogorov behavior is accompanied by a nonclassical self-preserving relation for the energy spectrum, i.e., $E = \epsilon L^3 f(kL)$, while the theoretical arguments of Bos and Rubinstein [13] (see also Refs. [18,19]) suggest that the slope of the energy spectrum exhibits a subdominant $-7/3$ deviation from the $-5/3$ equilibrium value [note that the equilibrium spectrum is $E \propto \epsilon^{2/3} L^{5/3} (kL)^{-5/3}$].

Evidently, near its initial conditions, the finite wave numbers of a decaying turbulence cascade achieve a particular organization, one which is not that of equilibrium, nor that of balance, pointing towards a nonclassical, but reproducible, evolution of turbulence at these early stages. The aim of this article is to derive analytical expressions for various flow quantities (i.e., interscale energy flux, kinetic energy, integral lengthscale) during this early stage, and shed some further light on the flow physics, in addition to the ones discussed in the previous works of Goto and Vassilicos [11] and Bos and Rubinstein [13]. The structure of the article is as follows. Section II briefly summarizes the recent discoveries on the evolution of out-of-equilibrium decaying turbulence. Section III derives a novel expression for the large-scale energy flux when the new dissipation scaling holds. Section IV explores the limitations of the recently proposed [11] early-decay energy spectrum expression $E = \epsilon L^3 f(kL)$. Section V combines the above two results (energy flux and energy spectrum expressions) to derive predictions of various flow quantities. Finally, Sec. VI provides a concluding summary. Throughout the paper, the various conclusions and intermediate steps of the analysis are validated using data from periodic box direct numerical simulations.

II. PRELIMINARY CONSIDERATIONS

In the ensuing analysis we consider homogenous turbulence and validate our conclusions using datasets of forced and decaying periodic box simulations (see Appendix A for the methodology details). The turbulence quantities that will be discussed are the kinetic energy of the cascade $K(t) \equiv \frac{3}{2}u^2 = \int_0^\infty E(k,t)dk$, the kinetic energy dissipation rate $\epsilon(t) = 2\nu \int_0^\infty k^2 E(k,t)dk$, the interscale energy flux Π , the integral lengthscale $L(t) = \frac{3\pi}{4} \int_0^\infty k^{-1} E(k,t)dk/K(t)$ and the Taylor microscale $\lambda = u\sqrt{15\nu/\epsilon}$, with $L/\lambda \gg 1$ for high Reynolds cascades. In the above, $E(k,t)$ is the three-dimensional energy spectrum. Given two lengthscales, we consider two Reynolds numbers, i.e., $\text{Re}_L = uL/\nu$ and $\text{Re}_\lambda = u\lambda/\nu$, with ν the kinematic viscosity. In the following, the subscript zero (for instance, in Re_{L0}) signifies that the quantity is either time-averaged in forced turbulence or corresponding to its ensemble-averaged value at the instant when the forcing is dropped for the decaying turbulence case. The superscript $>$ (for instance, in $K^>$) signifies that the integral quantity is high passed, i.e., it is integrated from wave number k to infinity. Having defined the important quantities, we now start with a brief description of some recent findings on the evolution of out-of-equilibrium cascades.

The direct numerical simulation (DNS) of Goto and Vassilicos [20] showed that, prior to the onset of decay, when homogenous turbulence is still steadily forced the flow quantities do not remain constant in time, but undergo intense quasiperiodical oscillations about a mean value [see, for instance, Ref. [21] and Fig. 9(b) in Appendix A]. It was also observed that these oscillations occur in such a way so that, at all times, dissipation follows the “new” scaling $\epsilon \propto u^2/L^2$, which can be readily shown [7] to be equivalent to $C_\epsilon \propto \text{Re}_\lambda^{-1}$ (using the definitions of $C_\epsilon = \epsilon L/u^3$ and the Taylor microscale). This trend can be seen in the appropriately plotted quantities of Fig. 1(a). After the forcing is removed and turbulence is left to decay, dissipation continues for some time to follow the new dissipation scaling. In experimental grid turbulence, this “initial” region occurs near the grid [see Fig. 1(b)]. At these initial transient stages, turbulence decays very abruptly and does not follow the milder power-law evolution that is known to characterize its later, “classical” region [22–25]. It is noteworthy that this steep “nonclassical” evolution also occurs at the early stages of eddy-damped quasinormal Markovian (EDQNM) decaying turbulence simulations and is thus not related to the

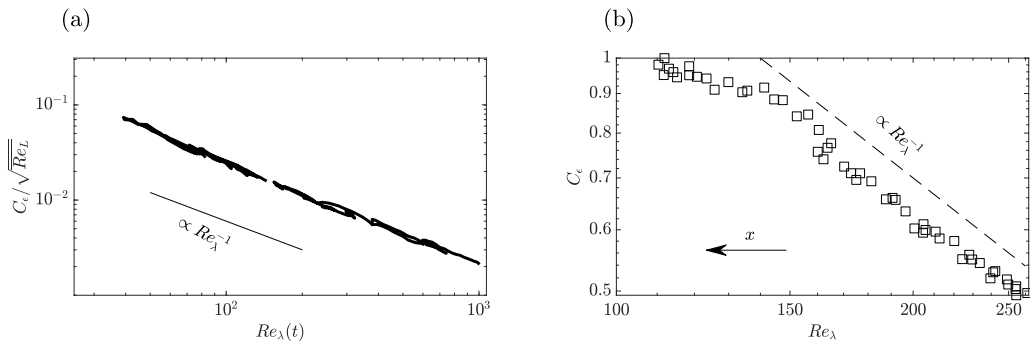


FIG. 1. Validation of the new dissipation scaling $C_\epsilon \propto Re_\lambda^{-1}$ using data from the literature. (a) Forced periodic box simulation data from Ref. [21]. Runs of different starting Re are plotted. (b) Decaying grid turbulence data from Ref. [16]. The arrow denotes an increasing distance from the grid. Note that at the distance corresponding to $Re_\lambda \approx 140$, the grid case shifts to $C_\epsilon = \text{const.}$

lack of homogeneity or anisotropy that might contaminate the early decay stages of experimental investigations [24].

When turbulence has sufficiently departed from its initial conditions (e.g., 10 to 15 mesh sizes downstream of the grid in experimental turbulence or a few turnover times after the onset of decay in DNS [11,14,16]), the dissipation scaling switches abruptly to the classical scaling, i.e., $\epsilon \propto u^3/L$, which is equivalent to $C_\epsilon = \text{const.}$ For instance, Fig. 1(b) shows that C_ϵ suddenly flattens at a critical distance downstream of a turbulence grid. Recent DNS and EDQNM simulations [11,24] suggest that, in decaying turbulence, the switching from the new to the classical dissipation scaling occurs when the initial “bump” in the energy spectrum disappears [see also Fig. 2(b)], while the flow model of Bos [26] suggests that the switching occurs when the initially dominant turbulence production term in the energy budget equation has sufficiently decayed.

Following this “switching,” homogenous turbulence enters its well-studied classical regime where decay occurs in a power-law manner [23,24] and $C_\epsilon = \text{const.}$ Steiros [12] recently showed that both these results occur because the cascade, far from its initial conditions, relaxes into a “balanced” nonequilibrium state where $\Pi_a/\epsilon = \text{const.}$, where the constant is less than unity, and

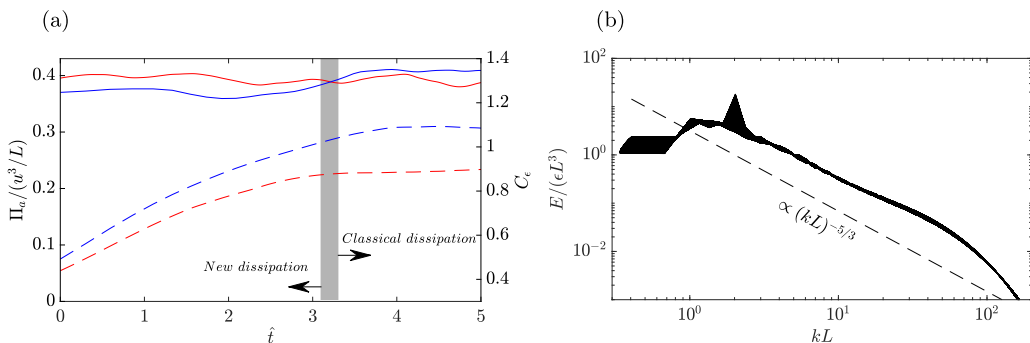


FIG. 2. (a) Normalized interscale energy flux of the largescales Π_a (solid lines) and dissipation coefficient (dashed lines) as a function of the number of turnover times since the stop of the forcing. Two DNS domain sizes are plotted, corresponding to “high” (red) and “low” (blue) Re (see Appendix A). The gray stripe marks the transition from the new to the classical dissipation scaling and corresponds to the neighborhood of the maximum value of dL^2/dt (see Sec. V). (b) Normalized power spectral density for the high Re case during the time that the new dissipation scaling holds ($\hat{t} < 3$).

where energy is “simply” transported in the cascade (see also the discussion in Bos *et al.* [9]). In the decaying DNS datasets used in this study [see Fig. 2(a)] the “new” dissipation scaling persists for approximately three turnover times (defined as $\hat{t} = \int_0^t u/L dt$) from the point the forcing stops ($t = 0$), after which the system shifts to $C_\epsilon = \text{const.}$ and the “balanced” regime.

III. LARGESCALE ENERGY FLUX

Consider the conventional cascade picture where, on average, large scales supply smaller ones with kinetic energy at a rate Π_a , eventually arriving to the dissipative scales where it is converted into heat. The demarcation between large scales and the rest of the cascade is assumed to occur at a normalized wave number $\kappa = \kappa_a$ of order unity with $\kappa = kL$. Given that cascade equilibrium and balance imply $\Pi_a/\epsilon \approx 1$ and $\Pi_a/\epsilon = \text{const.}$ (but less than unity), respectively, it is interesting to inspect how the ratio Π_a/ϵ behaves when the new dissipation scaling $\epsilon = Cu^2/L^2$ (equivalent to $C_\epsilon \propto \text{Re}_\lambda^{-1}$) holds. Note that, in the above expression, C is a constant with dimensions $[\text{m}^2\text{s}^{-1}]$. Its relationship with the system’s flow quantities is investigated below.

The rate of energy transfer from large scales is conventionally expressed as

$$\Pi_a = C_x u^3 / L, \quad (1)$$

where Π_a is evaluated at κ_a and C_x is a coefficient of proportionality. Figure 2(a) shows that expression (1) holds for decaying periodic-box turbulence if κ_a is taken shortly after the peak in the power spectral density [Fig. 2(b)], which is typically linked to large coherent structures. In particular, here Π_a is calculated for $\kappa_a \approx 3.3$, with the spectral peak being centered around $\kappa = 2$. The same expression has been shown to hold for forced turbulence as well [11,20]. The combination of expression (1) with the new dissipation scaling $\epsilon = Cu^2/L^2$ then yields the relation

$$\Pi_a/\epsilon = C_x u L / C.$$

The above expression is expected to hold for both forced and early decaying turbulence, i.e., while the effect of the initial conditions persists. The initial conditions should therefore appear in the above formula, i.e., in the constant C . To see that, we first consider the forced-case scenario, where a time averaging would yield $\bar{\epsilon} = \overline{\Pi_a}$, with the overline denoting the time-averaging operation (the large-scale dissipation is neglected). Moreover, we expect that the cascade time lag breaks any correlation between Π_a and Re_L in forced turbulence [see Fig. 10(b) in Appendix A for validation of this assumption]. Thus, time averaging of the above expression in the form $C_x \epsilon / C = \Pi_a / (uL)$, yields $C_x / C = \overline{(uL)^{-1}}$. This is approximately $C_x / C \approx \overline{uL}^{-1}$, i.e., $C \propto \overline{uL}$ (the forced turbulence data of Ref. [21] confirm this simplification). Consequently, the energy flux of the large scales becomes

$$\Pi_a/\epsilon = \frac{\text{Re}_L}{\text{Re}_{L0}}, \quad (2)$$

and using the formula $\Pi_a = C_x u^3 / L$ one obtains

$$\epsilon = C_x \overline{uL} \frac{u^2}{L^2}. \quad (3)$$

The derived prefactor \overline{uL} was empirically found in the forced turbulence DNS of Goto and Vassilicos [21] [see, for instance, Fig. 1(a)]. For decaying turbulence, we achieve a similar result if, instead of time averaging, we perform ensemble averaging at time $t = 0$, where turbulence is still forced. Thus, we have $\langle \epsilon \rangle = \langle \Pi_a \rangle$ at $t = 0$ and we obtain

$$\epsilon = C_x u_0 L_0 \frac{u^2}{L^2}, \quad (4)$$

which affirms the dependence of the constant to the initial conditions. Similarly to the forced case, the prefactor $u_0 L_0$ was found to be necessary to collapse the various decaying turbulence DNS runs

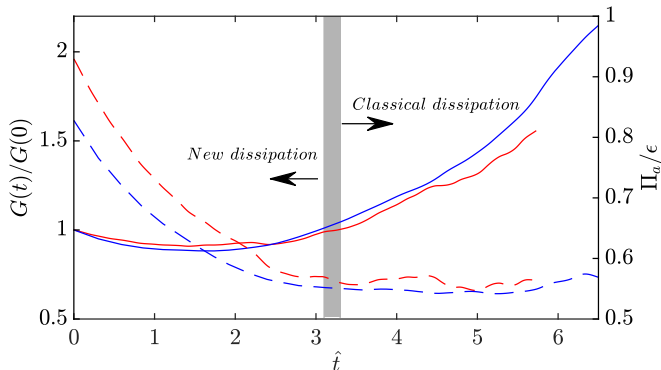


FIG. 3. Normalized parameter $G(t) = \Pi_a/(\epsilon \text{Re}_L)$ (solid lines) and Π_a/ϵ (dashed lines) as a function of the number of turnover times, for decaying periodic turbulence of high (red) and low (blue) Re (see Appendix A for numerical details) The gray stripe corresponds to neighborhood of $dL^2/dt = 0$, which marks the change of the dissipation scaling (see Sec. V).

in Ref. [11]. We also note that Bos and Rubinstein [13] proposed a link between the above expression and the nonequilibrium energy spectrum initially proposed in Ref. [19]. We thus conclude that, in close proximity to the initial conditions, a homogenous turbulence cascade (forced or decaying) exhibits the out-of-equilibrium behavior $\Pi_a/\epsilon = uL/u_0L_0$. To interpret the later expression, we may consider forced turbulence and combine expression (4) with Eq. (1) to obtain

$$\Pi_a \propto C_0 \epsilon^{3/2} L^2, \quad (5)$$

where $C_0 = (\nu u_0^{1/2} L_0^{1/2})^{-1}$. Any fluctuation of the left-hand side (energy flux), will cause a similar fluctuation in ϵ after a cascade time lag. However, in forced periodic box turbulence ϵ is found to be anticorrelated with L [see Fig. 10(a) in Appendix A] and thus, ϵ and L will move in opposite directions. Equation (5) then will resist any change in Π_a , suggesting a regulatory motion in the cascade that cancels fluctuations.

In summary, the interchangeable expressions $\epsilon \propto u_0 L_0 \frac{u^2}{L^2}$ and $\Pi_a = \epsilon u L / u_0 L_0$ hold until a critical time has passed in homogenous decaying turbulence and then the system shifts to the interchangeable expressions $\epsilon \propto u^3 / L$ and $\Pi_a \propto \epsilon$. The effect of initial conditions on the early decay regime is expressed through the coefficient $u_0 L_0$. The above are supported by the decaying turbulence DNS data used in this study, shown in Fig. 3. The physics behind $\Pi_a \propto \epsilon$ are understood (they express a spectral balance in the cascade, see, for instance, Ref. [12]). On the other hand, the physics behind the $\Pi_a = \epsilon u L / u_0 L_0$ are not perfectly understood, but were postulated to be linked to a spectral imbalance in the cascade (see Bos and Rubinstein [13]) and cascade regulation, possibly induced by the influence of the coherent structures in the flow (see Goto and Vassilicos [11]). Both of the above arguments are supported by the current work. In the following, we use the novel expression $\Pi_a/\epsilon = uL/u_0L_0$ to derive predictions for several integral quantities of the turbulence cascade, but before that, we investigate the limitations of a recently proposed energy spectrum scaling, valid for turbulence near initial conditions. It is noted that the scaling law $C_\epsilon \propto \text{Re}_\lambda^{-m}$ with $m = 1$ is used in this study. Small deviations from that value (for instance, $m = 15/14$ in Ref. [13]) are not expected to change the conclusions of this article drastically.

IV. ENERGY SPECTRUM

In accordance with the Kolmogorov theory, we might expect that as $\text{Re} \rightarrow \infty$ and $kL \rightarrow \infty$ the cascade approaches a state of equilibrium where $\Pi \approx \epsilon$. Indeed, the results of the authors of Refs. [27,28] indicate that unsteady cascades continually tend to equilibrium until a wave number $k = \mathcal{O}(\lambda^{-1})$, i.e., at large separations from L . At such small scales, dimensional analysis yields the

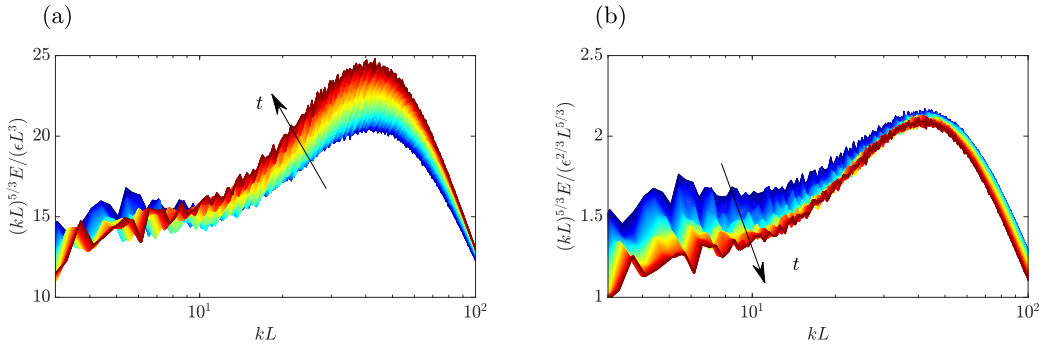


FIG. 4. Power spectral densities of the high-Re decaying periodic box dataset (see Appendix A for numerical details) normalized using (a) GGV’s compensation and (b) Kolmogorov’s compensation, while the new dissipation scaling holds ($\hat{t} < 3$). Warmer colors correspond to larger decay times.

equilibrium result $E \propto \epsilon^{2/3} L^{5/3} \kappa^{-5/3}$, with $\kappa = kL$ [6]. A natural question then is how the energy spectrum behaves at larger scales in unsteady turbulence, in between the integral lengthscale and the equilibrium scales of the cascade.

For the case of decaying homogenous turbulence far from initial conditions, Steiros [12] recently showed that the out-of-equilibrium scales of the cascade reach a state of “balance” where the energy spectrum evolves as $E \propto \epsilon^{2/3} L^{5/3} \kappa^{-5/3} g(\kappa)$, with $g(\kappa)$ a power-law correction which tends to unity (equilibrium) for increasing wave numbers. Closer to the initial conditions, however, the spectral balance and the corresponding correction are invalid. In that case, Goto and Vassilicos [11] provided evidence that the energy spectrum instead follows the self-preserving expression $E(k, t) \propto \epsilon L^3 f(\kappa)$ [see the reproduction of the data of Goto and Vassilicos in Fig. 2(b)]. This type of self-preservation can also be inferred from George’s earlier work [29] [see Eqs. (27) and (33) therein], and will be henceforth referred as George, Goto, and Vassilicos type (GGV) to distinguish it from the K41 self-similarity.

Figure 4 plots the energy spectra from the DNS dataset using a $-5/3$ compensation for the early decay times when the new dissipation scaling is still valid (the out-of-equilibrium early decay effects are expected to only slightly perturb the $-5/3$ slope, see Ref. [13]). The GGV compensation indeed provides a better collapse of the spectra than the K41 normalization at the relatively small wave numbers. However, at larger wave numbers (i.e., at the “bump” which is located at wave numbers of order λ^{-1}) the K41 normalization collapses the spectra better as equilibrium is being approached. In both cases, the discrepancy in the collapse [for higher wave numbers in Fig. 4(a) and lower wave numbers in Fig. 4(b)] is not random, but is exacerbated as decay progresses. The reason for that is explained in Appendix B.

The above arguments lead to the cascade picture shown in Fig. 5 where the energy spectrum follows the GGV self-similarity for $\kappa_a < \kappa < \kappa_b$, while larger normalized wave numbers are characterized by an approximate equilibrium. We note that in both George’s [29] and Goto and Vassilicos’ [11] works the GGV range was postulated to extend to and include the smallest, dissipative scales of the cascade. However, Figs. 4 and 6(a) show that (i) there is a tendency towards equilibrium at small scales (and thus the K41 inertial range scaling) and (ii) the even smaller, dissipative eddies evolve according to the universal Kolmogorov prediction [6], i.e., the GGV range is an out-of-equilibrium phenomenon, which is followed by the “universal” equilibrium range at smaller scales. Still, we note that a cascade equilibrium will form at scales of negligible size compared to that of the integral lengthscale, and thus the GGV range will extend to very large $\kappa = kL$, i.e., $\kappa_b \rightarrow \infty$, at high Reynolds number cascades.

We conclude this section by noting that the GGV-type self-similarity implies that the (relatively small) dissipation in the range $\kappa_a < \kappa < \kappa_b$ will be proportional to the total dissipation of the

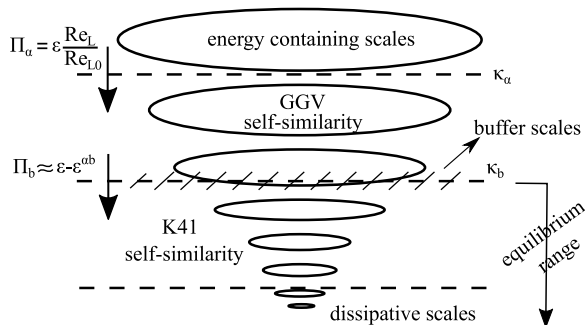


FIG. 5. Proposed cascade picture when the new dissipation scaling holds. Between large and small scales lies an intermediate range of scales which exhibits two types of self-similar behaviors: first a “GGV type” followed by a K41 type.

cascade, i.e., $\epsilon^{ab} \propto \epsilon$. This is readily demonstrated by taking the definition of dissipation for homogenous turbulence, i.e., $\epsilon^{ab} = 2\nu L^{-3} \int_{\kappa_a}^{\kappa_b} \kappa^2 E d\kappa$ (with $\kappa = kL$), and inserting $E \propto \epsilon L^3 f(\kappa)$. This result is validated in Fig. 6(b), where it is shown that, while the new dissipation scaling holds, the ratio ϵ^{ab}/ϵ stays relatively constant. A physical explanation for this behavior is that the majority of $\epsilon^{ab}(t)$ is expected to occur at the largest wave numbers of the GGv self-similar range, i.e., close to κ_b . The eddy turnover time at $\kappa \approx \kappa_b$ will thus regulate both ϵ^{ab} and Π_b , the latter being the energy flux at κ_b (see Fig. 5). We may thus expect that $\epsilon^{ab} \propto \Pi_b$ (i.e., that their ratio is time independent). Neglecting the dissipation of the large scales (i.e., for $\kappa < \kappa_a$) we have $\Pi_b \approx \epsilon - \epsilon^{ab}$ (i.e., equilibrium at κ_b). The combination of the above yields $\epsilon^{ab} = \Phi\epsilon$ with Φ a coefficient of proportionality when the new dissipation scaling is valid. We note that the integration boundaries κ_a and κ_b are expected to be time-invariant when the new dissipation scaling holds. For κ_a , this occurs because the GGv range starts immediately after the spectral peak [see Fig. 2(b)]. The DNS data show that, while the peak diminishes with time, it always stays centered around the same normalized wave number $\kappa = 2$. We thus expect κ_a to stay constant in time. At the same time, we might expect κ_b (i.e., the end of the GGv range) to be roughly proportional to L/λ , as argued above. Using the definition of the Taylor microscale, it can be readily shown that the new dissipation

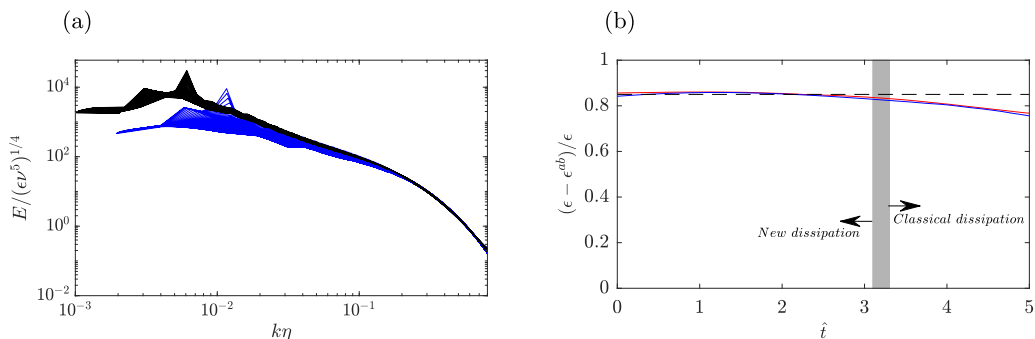


FIG. 6. (a) Periodic box DNS of decaying turbulence corresponding to two Reynolds numbers (high black and low blue, see Appendix A), plotted using Kolmogorov’s dissipation scaling. Both cases collapse as $k\eta \rightarrow 1$, with η being the Kolmogorov microscale. (b) Normalized dissipation against number of turnover times, for periodic box decaying turbulence. The threshold κ_b for the calculation of ϵ^{ab} is taken to be equal to 35 and 20 for the “high” (red line) and “low” (blue line) Reynolds number cases, respectively, which corresponds to the point where the GGv-type self-similarity has drastically deteriorated (see Fig. 4).

scaling $C_\epsilon \propto \text{Re}_\lambda^{-1}$ is equivalent to $L/\lambda = \text{const}$. Thus, it is expected that κ_b also stays constant in time when the new dissipation scaling holds.

V. CASCADE EVOLUTION

We now combine the previous two results (i.e., expressions for the large-scale energy flux and energy spectrum) to calculate several flow quantities of homogenous decaying turbulence near its initial conditions. We first integrate the Lin equation

$$\frac{\partial E(k, t)}{\partial t} = -\frac{\partial \Pi(k, t)}{\partial k} - 2\nu k^2 E(k, t),$$

from k to ∞ to obtain the scale-by-scale energy balance

$$\frac{\partial K^>}{\partial t} = \Pi - \epsilon^>. \quad (6)$$

The K41 equilibrium considers that the time-dependent term $\frac{\partial K^>}{\partial t}$ is negligible, leading to the usual equilibrium expression $\Pi \approx \epsilon$ (given that large-scale dissipation is very small). For scales which are not of negligible size, however, $\frac{\partial K^>}{\partial t}$ will not be close to zero in unsteady regimes and its evolution will determine the dynamics of turbulence.

By assuming a GGV-type self-similarity for the energy spectrum, Goto and Vassilicos [11] expanded $\frac{\partial K^>}{\partial t}$ and drew several conclusions regarding its evolution. Extending their analysis, here we will use the new expression $\Pi_a = \epsilon u L / u_0 L_0$ to “close” the energy budget equation and obtain predictions for several flow quantities.

Given the result of the previous section $\epsilon^{ab} = \Phi \epsilon$ we may obtain an expression for the coefficient of proportionality in the GGV energy spectrum expression $E = C' \epsilon L^3 f(\kappa)$. In particular, by using the definition of the dissipation for homogenous turbulence we have

$$L^{-3} \int_{\kappa_a}^{\kappa_b} 2\nu \kappa^2 C' \epsilon L^3 f(\kappa) d\kappa = \Phi \epsilon,$$

and thus, the consistent expression is

$$E(k, t) = \frac{\Phi \epsilon L^3}{2\nu I_2} f(\kappa), \quad (7)$$

where $I_2 = \int_{\kappa_a}^{\kappa_b} \kappa^2 f(\kappa) d\kappa$ is a constant, as both κ_a and κ_b are taken to be time invariant when the new dissipation scaling holds (see the last paragraph of the previous section). Integrating the above expression, we obtain the high-pass kinetic energy for wave numbers larger than k

$$K^>(k, t) = \frac{\Phi \epsilon L^2}{2\nu I_2} I_0(\kappa), \quad (8)$$

with $I_0(\kappa) = \int_{\kappa}^{\kappa_b} f(\kappa) d\kappa$. The above expression for $K^>$ assumes that $\kappa_b \rightarrow \infty$ even though we showed in the previous section that the dissipative scales cannot be included in the GGV range. However, given that $\kappa_b \gg 1$ and the drastic decrease in energy density with increasing wave numbers, the above expression can be thought to be an excellent approximation. By differentiating the above expression with respect to time one obtains

$$-\frac{I_2}{\Phi} \frac{\partial K^>}{\partial t} \frac{1}{\epsilon} = \frac{C_x \text{Re}_{L0} I_0(\kappa)}{3} + \frac{\kappa f(\kappa)}{4\nu} \frac{dL^2}{dt}, \quad (9)$$

where we used expression (4) for the term $d(\epsilon L^2)/dt$ and $dK/dt = d(\frac{3}{2}u^2)/dt = -\epsilon$. Expression (9) is essentially identical to the one derived by Goto and Vassilicos [11]. In the following, we combine it with the novel expression (2) to derive our predictions.

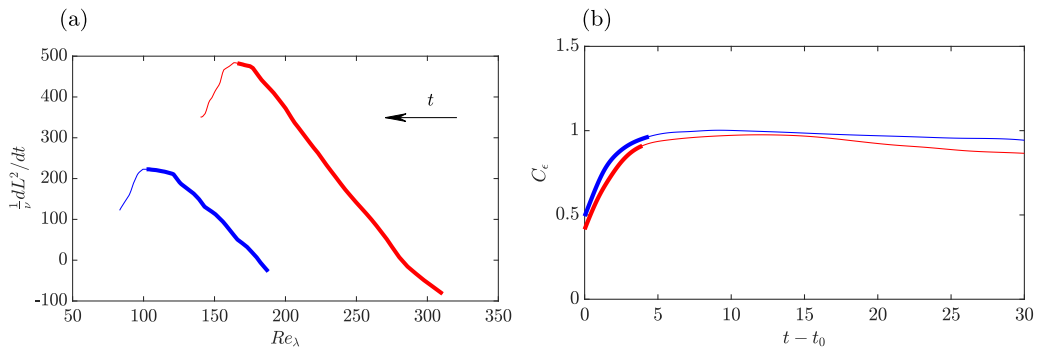


FIG. 7. (a) $\frac{1}{v} \frac{dL^2}{dt}$ and (b) C_ϵ for “high” (red) and “low” (blue) Re cases of decaying periodic box turbulence (the forcing stops at $t = t_0$). The thick part of the lines marks the range where $\frac{dL^2}{dt}$ grows.

A. Integral lengthscale

In the energy budget Eq. (6) the time-dependent term can be substituted by expression (9), evaluated at $\kappa = \kappa_a$. By noting that dissipation is negligible for $\kappa < \kappa_a$, $\epsilon^>$ can be also substituted with ϵ . To model the interscale energy flux Π_a , we utilize the novel expression (2). The result is an expression for dL^2/dt , i.e.,

$$\frac{1}{v} \frac{dL^2}{dt} = A - BRe_\lambda, \quad (10)$$

where $A = 4 \frac{I_2 \frac{1}{\Phi} - \frac{1}{3} C_x Re_{L0} I_0}{\kappa_a f(\kappa_a)}$ and $B = \frac{4I_2}{\Phi \kappa_a f(\kappa_a)} \sqrt{\frac{C_x}{15 Re_{L0}}}$ are positive constants dependent on the initial conditions (note that the definition of the Taylor microscale was also used).

Equation (10) will be valid in the early decay, while turbulence follows the new dissipation scaling. After turbulence has transitioned to the classical dissipation scaling, the cascade will evolve in a “balanced” state [11,12] where the classical dissipation scaling holds and an equation resembling the ϵ equation of the $k - \epsilon$ can be derived (see Steiros [12]), i.e.,

$$\frac{d\epsilon}{dt} = -C_0 \frac{\epsilon^2}{\frac{3}{2} u^2},$$

where C_0 can be calculated by assuming a turbulence invariant (e.g., $C_0 = 1.7$ for Loitsyanskii’s and $C_0 = 1.83$ for Saffman’s invariants [12]). By inserting the classical dissipation scaling $\epsilon = C_\epsilon u^3/L$ (valid in the balanced decay [11,12]) to the above expression and using the definition of the Taylor microscale $\lambda = u \sqrt{15\nu/\epsilon}$ one obtains

$$\frac{1}{v} \frac{dL^2}{dt} = B' Re_\lambda^2, \quad (11)$$

with $B' = \frac{2C_\epsilon^2}{15} (\frac{2}{3} C_0 - 1)$ a positive constant for both Saffman’s and Loitsyanskii’s invariants (note that the current DNS datasets were found to be very close to Loitsyanskii’s invariant). By comparing Eqs. (10) (for the early decay) and (11) (for the later, balanced decay) we may conclude that the transition from the new to the classical dissipation scaling occurs when the slope of $\frac{dL^2}{dt}$ changes sign. The above is validated in Fig. 7(a) using the two decaying periodic box datasets. In accordance with Eq. (10), $\frac{dL^2}{dt}$ is a linear decreasing function of Re_λ , for as long as the new dissipation scaling holds [see Fig. 7(b)]. When the system transitions to the classical scaling (i.e., $C_\epsilon = \text{const.}$), $\frac{dL^2}{dt}$ becomes an increasing function of Re_λ , in agreement with Eq. (11). The maximum value of $\frac{dL^2}{dt}$ marks the state change.

B. Turbulence kinetic energy

By combining expressions (4) and (10) we may obtain an expression for the evolution of the turbulent kinetic energy during decay when the new dissipation scaling holds. The elimination of time yields (the definition of the Taylor microscale $\lambda^2 = 15\nu u^2/\epsilon$ is also used)

$$\frac{du^2}{dL^2} = \frac{-u^2}{C_1 L^2 - C_2 u L^3}, \quad (12)$$

where $C_1 = \frac{6I_2/(\Phi \text{Re}_{L0} C_x) - 2I_0}{\kappa_a f(\kappa_a)}$ and $C_2 = \frac{6I_2}{\Phi \kappa_a f(\kappa_a) \text{Re}_{L0} C_x u_0 L_0}$. It can be checked by substitution that a solution to the above equation is

$$\frac{C_1 - 1}{uL} = C_2 - \left(\frac{u}{C}\right)^{C_1-1}, \quad (13)$$

with C a positive constant of integration. The combination of Eqs. (4) and (13) yields the generalized logistic equation [30]

$$\frac{du^2}{dt} \propto -u^4 \left[1 - \left(\frac{u}{c}\right)^{C_1-1}\right]^2, \quad (14)$$

with c a positive constant. Evidently, at the initial stages of decay when the new dissipation scaling holds, the kinetic energy will not follow a power law, in agreement with the EDQNM simulations of Ref. [24].

C. Interscale energy flux

In the previous section we derived expression (10) for dL^2/dt . Using the definition of the Taylor microscale, it becomes

$$\frac{1}{v} \frac{dL^2}{dt} = \frac{4}{3} \frac{C_x I_0(\kappa_a) \text{Re}_{L0}}{\kappa_a f(\kappa_a)} \left(\frac{1}{\Psi} - 1 - \frac{1}{\Psi} \frac{\text{Re}_L}{\text{Re}_{L0}} \right),$$

where $\Psi = \Phi \text{Re}_{L0} C_x I_0(\kappa_a)/(3I_2)$ is a constant. By inserting the above to expression (9) and using Ψ to substitute I_2 we obtain

$$\frac{1}{\epsilon} \frac{\partial K^>}{\partial t} = -\Psi \frac{I_0(\kappa)}{I_0(\kappa_a)} - \frac{\kappa f(\kappa)}{\kappa_a f(\kappa_a)} \left(1 - \Psi - \frac{\text{Re}_L}{\text{Re}_{L0}} \right).$$

To estimate $I_0(\kappa) = \int_{\kappa}^{\kappa_b} f(\kappa) d\kappa$ and $\kappa f(\kappa)$ we may assume that the energy spectrum follows, approximately, a power law in the GGV self-similar range, i.e., $f(\kappa) \propto \kappa^{-p}$. The recent results of Ref. [13] showed that, when the new dissipation scaling holds, the spectral slope will be only minimally perturbed from the equilibrium value $p = 5/3$, as also suggested by the DNS data of Fig. 2(b). For large Reynolds numbers we expect $\kappa_b \rightarrow \infty$, and given the power-law behavior of $f(\kappa)$ the above expression is simplified to

$$\frac{1}{\epsilon} \frac{\partial K^>}{\partial t} \approx -\left(\frac{\kappa}{\kappa_a}\right)^{1-p} \left(1 - \frac{\text{Re}_L}{\text{Re}_{L0}}\right),$$

which yields an asymptotic stationarity of $K^>$ as κ grows larger than κ_a . Noting that $\frac{\partial K^>}{\partial t} = \Pi - \epsilon$, the above expression becomes

$$\frac{\Pi}{\epsilon} \approx 1 - \left(\frac{\kappa}{\kappa_a}\right)^{1-p} \left(1 - \frac{\text{Re}_L}{\text{Re}_{L0}}\right), \quad (15)$$

for $\kappa \geq \kappa_a$ and p close to $5/3$. Equation (15) predicts equilibrium (i.e., $\Pi \approx \epsilon$) in two cases: first for asymptotically small scales (i.e., for $\kappa/\kappa_a \rightarrow \infty$) at any time. Second, at the initial time $t_0 = 0$ (i.e., when $\text{Re}_L = \text{Re}_{L0}$), at any wave number. The second case of equilibrium occurs because both Π and ϵ are ensemble-averaged and at $t = 0$ the cascade is still forced. Conservation of energy

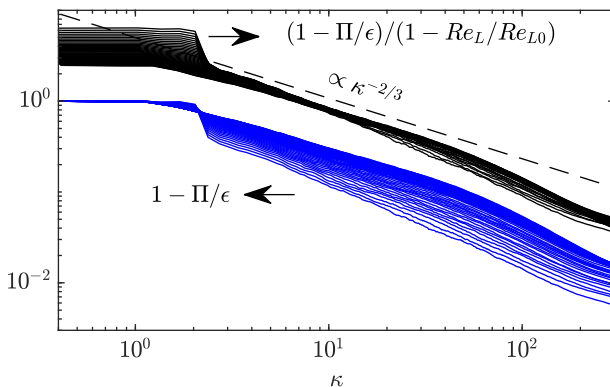


FIG. 8. Validation of expression (15) using the high-Re decaying turbulence DNS, for $\hat{t} < 3$. The Re_{L0} is appropriately corrected, as explained in the text. The dissipation is calculated as $2\nu L^{-3} \int_{\kappa}^{\infty} \kappa^2 E d\kappa$.

dictates that a forced turbulence cascade which is free to explore all possible states, will be, on average, in equilibrium.

However, Fig. 3 shows that for $\kappa = \kappa_a$ the interscale flux is slightly smaller than the dissipation at $t_0 = 0$ (e.g., $\Pi_a/\epsilon = 0.92$ for the high Reynolds case). This small discrepancy is probably due to insufficient ensemble averaging in the DNS (see Ref. [11]), which naturally is not an issue in experimental grid turbulence. The repercussion is that the Reynolds number of the DNS dataset at $t_0 = 0$ will not correspond to the properly averaged Re_{L0} value that Eq. (15) requires. Nevertheless, we may obtain a correction for $Re_L(t_0)$ in the following way: we note that, in an appropriately averaged cascade, at the initial instant of decay (where turbulence is still forced) an ensemble-averaged equilibrium is expected, i.e., $\Pi_a = \epsilon$ at $Re_L = Re_{L0}$ and $\kappa = \kappa_a$. Given then that at $t = 0$ we have $\Pi_a = 0.92\epsilon$, Eq. (15) yields a “corrected” initial condition $Re_{L0} = Re_L(t_0)/0.92$, where $Re_L(t_0)$ is the improperly averaged Reynolds number that we measure in the DNS dataset.

Figure 8 validates expression (15) for the time when the new dissipation scaling is valid (i.e., $\hat{t} < 3$). The spectra collapse after $\kappa_a \approx 3$, supporting the validity of expression (15). $Re_L(t_0)$ is corrected as described in the previous paragraph (i.e., multiplied by $1/0.92$), but we note that this correction improves the collapse only slightly. The slope was found to be close to $-2/3$, a further indication that, at the early stages of decay, the energy spectra are only slightly perturbed from the equilibrium $-5/3$ exponent, as predicted in Ref. [13]. It is noteworthy to mention that the standard expression $1 - \Pi/\epsilon$, which is expected to describe the interscale energy flux during equilibrium or balanced nonequilibrium decay [6,12], does not produce an acceptable collapse of the curves.

VI. CONCLUDING REMARKS

This work presents a theoretical and numerical investigation of homogenous turbulence near initial conditions when the new dissipation scaling $\epsilon \propto u_0 L_0 u^2 / L^2$ holds. This occurs when homogenous turbulence is still forced, or shortly after the forcing is removed. Under these conditions, it is shown that the large-scale energy flux Π_a obeys a nonequilibrium relation, while the nonequilibrium portion of the spectrum (but for smaller scales than the integral lengthscale) evolves in a nonclassical self-preserving manner. By combining these two expressions (i.e., for the energy flux and energy spectrum), nonequilibrium formulas for the integral lengthscale, turbulence kinetic energy, and energy flux across scales are derived whose predictions are supported by data from DNS of homogenous decaying turbulence. It is hoped that these expressions will prove useful when deriving turbulence model corrections for out-of-equilibrium effects.

After a critical time has passed from the onset of decay, turbulent dissipation transitions to its classical scaling. The transition is quite abrupt and is shown to occur at the location where the

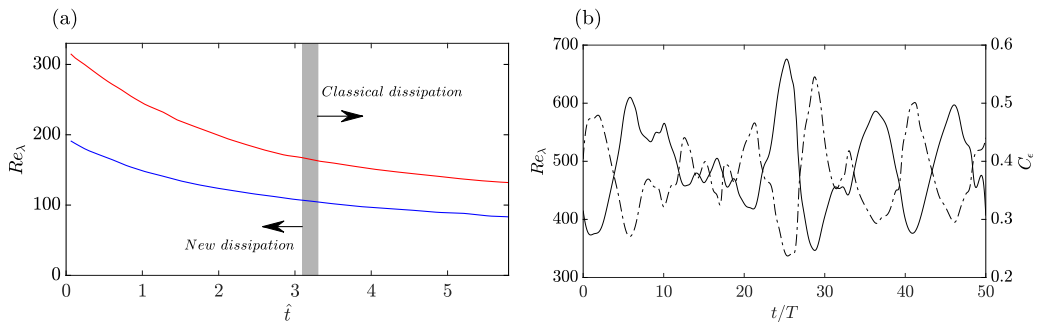


FIG. 9. (a) Decay of Re_λ versus number of turnover times for decaying periodic box turbulence of domain size $N = 2048$ (red) and $N = 1024$ (blue) (from Ref. [11]). (b) Evolution of Re_λ (solid line) and C_ϵ (dashed-dotted line) for periodic box turbulence of constant forcing versus time normalized with the mean turnover time (from Ref. [21]). Note the quasiperiodical oscillations.

second derivative of the square of the integral lengthscale changes sign. After that point, turbulence follows a “balanced” decay, described in the works of Refs. [11] and [12].

ACKNOWLEDGMENTS

Many thanks are due to S. Goto for generously providing the DNS data, and to J. C. Vassilicos for useful discussions and for reading an early version of the manuscript. The author was supported by an Imperial College London Junior Research Fellowship.

APPENDIX A: VALIDATION DATASETS

For validation purposes, two datasets of periodic-box decaying turbulence are used, the details of which are presented in Ref. [11]. For both cases, a forcing $f = [-\sin(k_f x) \cos(k_f y), \cos(k_f x) \sin(k_f y), 0]$ with $k_f = 4$ is imposed on the Navier-Stokes equations and is turned off at $t = t_0$, allowing the turbulence to decay. The first dataset concerns an ensemble of ten simulations of $N^3 = 1024^3$; the presented results are ensemble averages. The second dataset concerns a simulation size of $N^3 = 2048^3$ that contains a single run. The larger simulation size corresponds to a larger Reynolds number. The spatial resolution $k_{\max} \eta$ is slightly larger than the one at t_0 , while $k_{\max} \eta$ increases during decay. The decay of Re_λ for the two datasets is depicted in Fig. 9(a).

Additionally, data were retrieved from Ref. [21], for the case of steadily forced periodic-box simulations. The flow quantities underwent quasiperiodic oscillations [see, for instance, Fig. 9(b)] where Re_λ and C_ϵ oscillate in anticorrelation, in accordance with the new dissipation scaling of Eq. (3). In that case, ϵ and Re_L were found to be slightly anticorrelated [see Fig. 10(a)], whereas the large-scale interscale flux Π_a and Re_L did not exhibit signs of correlation [see Fig. 10(b)].

APPENDIX B: TIME DEPENDENCE OF SPECTRA IN FIG. 4

Given the new dissipation scaling $\epsilon \propto u^2/L^2$, the GGV and Kolmogorov self-similarities are connected via the identity

$$\underbrace{\frac{E}{\epsilon^{2/3} L^{5/3}}}_{\text{K41-type}} \propto \underbrace{\frac{E}{\epsilon L^3}}_{\text{GGV-type}} Re_L^{2/3}.$$

The above expression makes clear that if the GGV-type normalization is valid (i.e., $E/\epsilon L^3$ is constant in time), the K41-type normalization cannot be constant with time, but will instead produce curves which have a decreasing value as Reynolds number decreases, i.e., as time increases (given

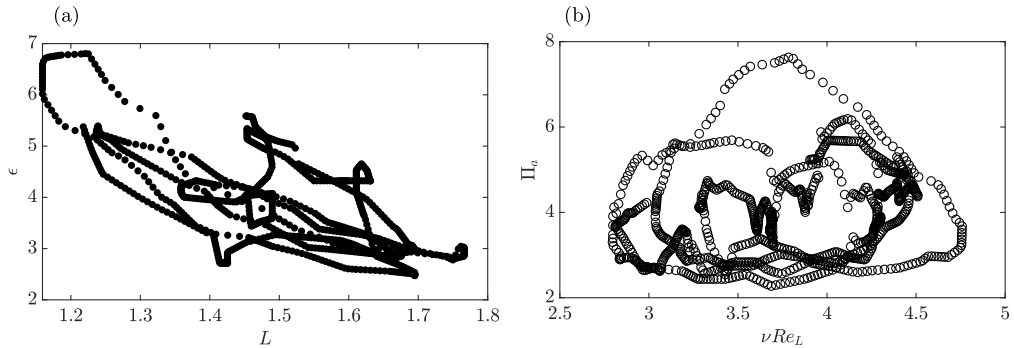


FIG. 10. (a) Dissipation versus integral lengthscale and (b) large-scale flux versus Re_L , for the forced turbulence simulation shown in Fig. 9(b).

the turbulence decay). This is indeed observed in Fig. 4(b) at low wave numbers. The opposite occurs when the K41-type normalization is valid [see Fig. 4(a) at high wave numbers]: in that case, the GGV-type normalization leads to higher values as time progresses.

-
- [1] G. K. Batchelor, *The Theory of Homogeneous Turbulence* (Cambridge University Press, Cambridge, England, 1953).
 - [2] K. R. Sreenivasan, On the scaling of the turbulence energy dissipation rate, *Phys. Fluids* **27**, 1048 (1984).
 - [3] A. N. Kolmogorov, Dissipation of energy in the locally isotropic turbulence, *Dokl. Akad. Nauk SSSR A*, **32**, 16 (1941).
 - [4] A. N. Kolmogorov, The local structure of turbulence in incompressible viscous fluid for very large Reynolds numbers, *Dokl. Akad. Nauk SSSR A*, **30**, 301 (1941).
 - [5] A. N. Kolmogorov, On degeneration (decay) of isotropic turbulence in an incompressible viscous fluid, *Dokl. Akad. Nauk SSSR A*, **31**, 538 (1941).
 - [6] S. B. Pope, *Turbulent Flows* (IOP, Bristol, England, 2001).
 - [7] J. C. Vassilicos, Dissipation in turbulent flows, *Annu. Rev. Fluid Mech.* **47**, 95 (2015).
 - [8] T. Ishihara, T. Gotoh, and Y. Kaneda, Study of high-reynolds number isotropic turbulence by direct numerical simulation, *Annu. Rev. Fluid Mech.* **41**, 165 (2009).
 - [9] W. J. T. Bos, L. Shao, and J. P. Bertoglio, Spectral imbalance and the normalized dissipation rate of turbulence, *Phys. Fluids* **19**, 045101 (2007).
 - [10] J. L. Lumley, Some comments on turbulence, *Phys. Fluids* **4**, 203 (1992).
 - [11] S. Goto and J. C. Vassilicos, Unsteady turbulence cascades, *Phys. Rev. E* **94**, 053108 (2016).
 - [12] K. Steiros, Balanced nonstationary turbulence, *Phys. Rev. E* **105**, 035109 (2022).
 - [13] W. J. T. Bos and R. Rubinstein, Dissipation in unsteady turbulence, *Phys. Rev. Fluids* **2**, 022601(R) (2017).
 - [14] J. Isaza, R. Salazar, and Z. Warhaft, On grid-generated turbulence in the near-and far field regions, *J. Fluid Mech.* **753**, 402 (2014).
 - [15] F. Liu, L. P. Lu, W. J. T. Bos, and L. Fang, Assessing the nonequilibrium of decaying turbulence with reversed initial fields, *Phys. Rev. Fluids* **4**, 084603 (2019).
 - [16] P. Valente and J. C. Vassilicos, Universal Dissipation Scaling for Nonequilibrium Turbulence, *Phys. Rev. Lett.* **108**, 214503 (2012).
 - [17] M. Waławczyk, J. L. Nowak, H. Siebert, and S. P. Malinowski, Detecting non-equilibrium states in atmospheric turbulence, *Journal of the Atmospheric Sciences* **79**, 2757 (2022).
 - [18] K. Horiuti and T. Tamaki, Nonequilibrium energy spectrum in the subgrid-scale one-equation model in large-eddy simulation, *Phys. Fluids* **25**, 125104 (2013).

- [19] A. Yoshizawa, Nonequilibrium effect of the turbulent-energy-production process on the inertial-range energy spectrum, *Phys. Rev. E* **49**, 4065 (1994).
- [20] S. Goto and J. C. Vassilicos, Energy dissipation and flux laws for unsteady turbulence, *Phys. Lett. A* **379**, 1144 (2015).
- [21] S. Goto and J. C. Vassilicos, Local equilibrium hypothesis and Taylor's dissipation law, *Fluid Dynamics Research* **48**, 021402 (2016).
- [22] L. B. Esteban, J. S. Shrimpton, and B. Ganapathisubramani, Laboratory experiments on the temporal decay of homogeneous anisotropic turbulence, *J. Fluid Mech.* **862**, 99 (2019).
- [23] P. Å. Krogstad and P. A. Davidson, Near-field investigation of turbulence produced by multi-scale grids, *Phys. Fluids* **24**, 035103 (2012).
- [24] M. Meldi and P. Sagaut, Investigation of anomalous very fast decay regimes in homogeneous isotropic turbulence, *J. Turbul.* **19**, 390 (2018).
- [25] S. R. Yoffe and W. D. McComb, Onset criteria for freely decaying isotropic turbulence, *Phys. Rev. Fluids* **3**, 104605 (2018).
- [26] W. J. T. Bos, Production and dissipation of kinetic energy in grid turbulence, *Phys. Rev. Fluids* **5**, 104607 (2020).
- [27] T. S. Lundgren, Kolmogorov turbulence by matched asymptotic expansions, *Phys. Fluids* **15**, 1074 (2003).
- [28] M. Obligado and J. C. Vassilicos, The non-equilibrium part of the inertial range in decaying homogeneous turbulence, *Europhys. Lett.* **127**, 64004 (2019).
- [29] W. K. George, The decay of homogeneous isotropic turbulence, *Phys. Fluids* **4**, 1492 (1992).
- [30] A. Tsoularis and J. Wallace, Analysis of logistic growth models, *Mathematical Biosciences* **179**, 21 (2002).